

## Surface metallic states in ultrathin Bi(001) films studied with terahertz time-domain spectroscopy

K. Yokota, J. Takeda, C. Dang, G. Han, D. N. McCarthy et al.

Citation: *Appl. Phys. Lett.* **100**, 251605 (2012); doi: 10.1063/1.4729149

View online: <http://dx.doi.org/10.1063/1.4729149>

View Table of Contents: <http://apl.aip.org/resource/1/APPLAB/v100/i25>

Published by the [American Institute of Physics](#).

---

### Related Articles

Graphene on Rh(111): Scanning tunneling and atomic force microscopies studies

*Appl. Phys. Lett.* **100**, 241606 (2012)

Ambipolar charge injection and transport of few-layer topological insulator Bi<sub>2</sub>Te<sub>3</sub> and Bi<sub>2</sub>Se<sub>3</sub> nanoplates

*J. Appl. Phys.* **111**, 114312 (2012)

High resolution synchrotron radiation based photoemission study of the in situ deposition of molecular sulphur on the atomically clean InGaAs surface

*J. Appl. Phys.* **111**, 114512 (2012)

Study on spin-splitting phenomena in the band structure of GdN

*Appl. Phys. Lett.* **100**, 232410 (2012)

Interfacial layer growth condition dependent carrier transport mechanisms in HfO<sub>2</sub>/SiO<sub>2</sub> gate stacks

*Appl. Phys. Lett.* **100**, 232903 (2012)

---

### Additional information on *Appl. Phys. Lett.*

Journal Homepage: <http://apl.aip.org/>

Journal Information: [http://apl.aip.org/about/about\\_the\\_journal](http://apl.aip.org/about/about_the_journal)

Top downloads: [http://apl.aip.org/features/most\\_downloaded](http://apl.aip.org/features/most_downloaded)

Information for Authors: <http://apl.aip.org/authors>

## ADVERTISEMENT



**Agilent Technologies**

### Agilent Education and Research Resources DVD 2012

Packed with over **100 NEW** articles, application notes, webcasts, and videos relating to Renewable Energy, Nanoscience, RF/Wireless, MIMO, Materials, Digital Signals, Photonics, and General Test & Measurement.

Click Here to  
Order Your DVD



Agilent Technologies

## Surface metallic states in ultrathin Bi(001) films studied with terahertz time-domain spectroscopy

K. Yokota,<sup>1</sup> J. Takeda,<sup>1</sup> C. Dang,<sup>2</sup> G. Han,<sup>2</sup> D. N. McCarthy,<sup>2</sup> T. Nagao,<sup>2</sup> S. Hishita,<sup>3</sup> M. Kitajima,<sup>4</sup> and I. Katayama<sup>1</sup>

<sup>1</sup>Department of Physics, Graduate School of Engineering, Yokohama National University, Yokohama 240-8501, Japan

<sup>2</sup>WPI-MANA, National Institute for Materials Science, Tsukuba 305-0044, Japan

<sup>3</sup>Environment and Energy Materials Division, National Institute for Materials Science, Tsukuba 305-0044, Japan

<sup>4</sup>Department of Applied Physics, National Defense Academy, Yokosuka 239-8686, Japan

(Received 13 April 2012; accepted 27 May 2012; published online 19 June 2012)

Dynamical response of surface metallic states in single crystalline ultrathin Bi(001) films on Si(111)  $7 \times 7$  surface was investigated at a spectral range of 0.1–12 THz by broadband terahertz time-domain spectroscopy. The observed transmittance increased with a decrease in the thickness, without showing a gap structure. The measured complex dielectric dispersion was analyzed using a Drude model, and the plasma frequency ( $\omega_p$ ) and damping constant ( $\gamma$ ) were found to be inversely proportional to the thickness. The results strongly indicate the existence of surface metallic states, whose carrier density and damping constant are estimated to be  $3.08 \times 10^{19} \text{ cm}^{-3}$  and  $4.83 \times 10^2 \text{ THz}$ , respectively. © 2012 American Institute of Physics. [<http://dx.doi.org/10.1063/1.4729149>]

Semimetal bismuth (Bi) is one of the most extensively studied materials in condensed matter physics, because it exhibits many unique physical properties, for example, it has the highest electrical conductivity and magneto resistance among all metals. These properties are attributed to be unique electronic structure of semimetal Bi, such as a long Fermi wavelength (30–40 nm) and a very small effective electron mass. Recently, surfaces and thin films of Bi have attracted increasing interest because of the large spin-orbit coupling effect of Bi; this effect gives rise to characteristic surface metallic states with large spin-orbit splitting arising from the loss of the inversion symmetry at the surface (Rashba effect).<sup>1–3</sup> These metallic states are directly related to the topological insulators, such as  $\text{Bi}_{1-x}\text{Sb}_x$  alloys ( $0.07 < x < 0.22$ )<sup>4–6</sup> as well as of Bi bilayers (BLs).<sup>7,8</sup> Owing to spin splitting, the surface states of ultrathin films could be one of the platforms for transmitting the spin current, which is currently attracting significant interests for spintronics applications.

The long mean free path and small density of states at the Fermi level in Bi give rise to characteristic phenomena in nanoscale ultrathin films, such as: the quantization of the electronic states along the direction of thickness of the films and oscillatory conductivity as a function of the thickness of the films.<sup>9</sup> Theoretically, the quantization was expected to originate semimetal-to-semiconductor (SMSC) transition, which will occur at a thickness of 20–30 nm;<sup>10,11</sup> on the other hand, several authors have reported that the surface metallic state hinders the SMSC transition in ultrathin Bi films.<sup>12,13</sup> Furthermore, carrier dynamics of the electronic states in ultrathin Bi films has not fully been understood. Therefore, a new reliable method to observe the surface electronic state is indispensable for understanding the physical properties of ultrathin Bi films.

In this Letter, we show that broadband terahertz time-domain spectroscopy (THz-TDS) is an effective method for revealing the surface electronic states and the carrier dynam-

ics in ultrathin Bi films. Both the surface metallic state and the semimetal bulk states show a Drude-like response, whereas the SMSC transition gives rise to a gap structure in the terahertz frequency region ( $\sim 40 \text{ meV}$ , 9.7 THz).<sup>10,11</sup> We measured the transmittance of ultrathin Bi films with thicknesses in the range of 2.8–40 nm and obtained the complex dielectric dispersion of the films for each value of thickness in the range of 0.1–12 THz. Further, we analyzed dispersion using a Drude model, and quantitatively evaluated the plasma frequency, carrier density, and damping constant. The obtained high carrier density ( $3.1 \times 10^{19} \text{ cm}^{-3}$ ) clearly shows the existence of a surface metallic state, and the large damping constant ( $4.8 \times 10^2 \text{ THz}$ ) indicates the effective surface scattering such as carrier-carrier scattering. Because the physical parameters for the surface metallic states can be independently evaluated, the broadband THz-TDS has a great advantage over conventional techniques such as the DC conductivity measurement, which only detects the product of the carrier density and the damping constant.

Single crystalline ultrathin Bi(001) films were grown in an ultrahigh vacuum chamber ( $\leq 4 \times 10^{-9} \text{ Torr}$ ) at room temperature and characterized *in situ* using reflection high-energy electron diffraction.<sup>14</sup> Bi was deposited on a clean Si(111)- $7 \times 7$  surface, which was prepared by DC resistive heating at  $\sim 1500 \text{ K}$ . One bilayer (BL) has a thickness of 3.9 Å in the Bi(001) plane. The Bi deposition rate was calibrated by *ex situ* Rutherford backscattering experiments. After the Bi(001) films were deposited, they were annealed at  $\sim 350 \text{ K}$  to obtain atomically flat films.<sup>15</sup> We prepared ultrathin Bi(001) films with different thicknesses ranging from 2.8 to 40 nm. The film samples were transferred to a sample chamber (pumped down to  $10^{-6} \text{ Torr}$ ) in the broadband THz-TDS system within 10 h after they were prepared. We observed the film transmittance at room temperature in the range of 0.1–12 THz using the THz-TDS system. Details of the system were described previously.<sup>16</sup>

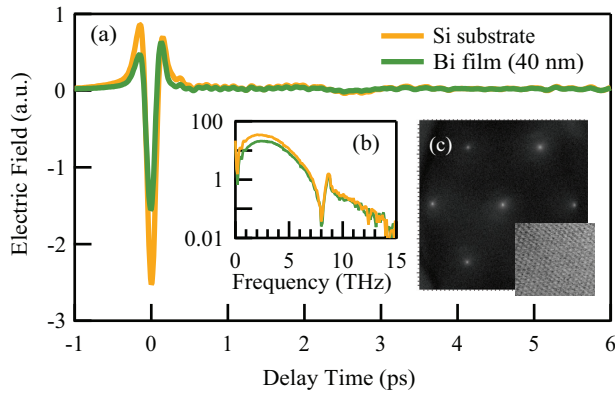


FIG. 1. (a) Temporal waveforms of the terahertz wave transmitted through an ultrathin Bi(001) film with a thickness of 40 nm and a referential Si substrate. (b) Amplitude spectra obtained by Fourier transformation. (c) LEED pattern obtained from the 40-nm-thick Bi(001) film and the scanning tunneling micrograph of the same film obtained from a  $7.7 \times 7.7 \text{ nm}^2$  area (lower-right inset).

Figure 1(a) shows the temporal profiles of the terahertz wave transmitted through an ultrathin Bi(001) film with a thickness of 40 nm and a referential Si substrate. Figure 1(b) shows the amplitude spectra obtained by Fourier transformation. The ratio of the transmittance of the ultrathin Bi(001) film to that of the referential Si decreases with an increase in the thickness over the entire frequency range up to 5 THz.

Figure 1(c) shows the low-energy electron diffraction (LEED) pattern and the scanning tunneling micrograph (STM) for the ultrathin Bi(001) film with a thickness of 40 nm. The LEED result shows several sharp diffraction spots, indicating that this film exhibits high crystallinity. The STM image indicates that Bi atoms are regularly arranged at the surface of the thin film. The surface roughness estimated by the atomic force microscope measurement was less than several nanometers, indicating that the film has a wide flat area. Therefore, the surface of the Bi film at which the terahertz wave transmitted can be treated as uniform.

Figure 2(a) shows the transmittance spectra of ultrathin Bi(001) films with different thicknesses ranging from 2.8 to 40 nm. The transmittance increases with a decrease in the thickness, and the transmittance for each value of thickness gradually decreases toward the lower frequency. Stronger absorption in a low frequency region within a spectral range of 0.1–12 THz suggests that no gap structure was observed in ultrathin Bi(001) films. In order to discuss the electronic structure of ultrathin Bi(001) films in detail, we calculated the sheet dielectric constant of ultrathin Bi(001) films using the following formula:<sup>17,18</sup>

$$\epsilon(\omega) = \frac{i(n_2 + 1)c}{\omega d} \frac{1 - T/T_0}{T/T_0}. \quad (1)$$

Here,  $n_2$  is the dielectric constant of Si,  $d$  the thickness of the ultrathin Bi(001) film, and  $T/T_0$  the complex transmittance of the Bi film relative to that of the referential Si substrate.

Figure 2(b) shows the real and imaginary parts of the complex dielectric constant for ultrathin Bi(001) films with a thickness of 40 nm. Because of the absence of the gap struc-

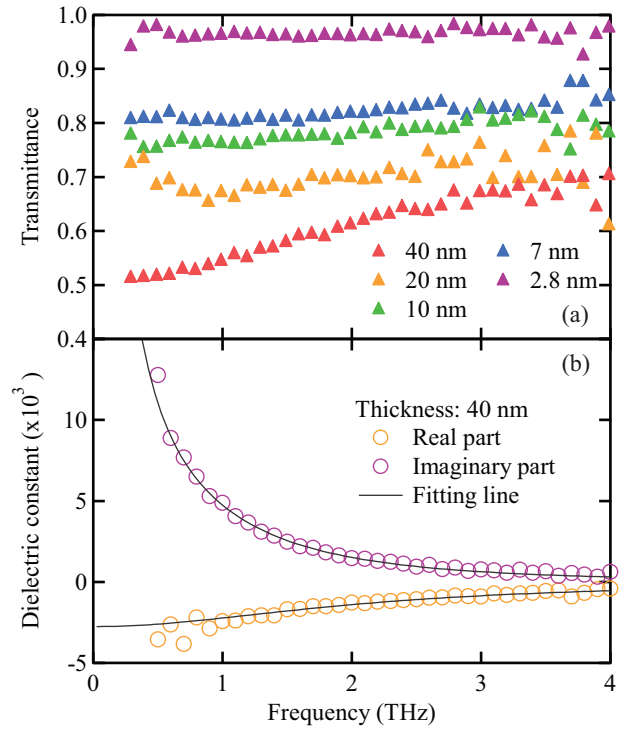


FIG. 2. (a) Transmittance of ultrathin Bi(001) films with thickness in the range of 2.8–40 nm. (b) The real and imaginary parts of the complex dielectric dispersion observed for an ultrathin Bi(001) film with a thickness of 40 nm (circles), and the fitting lines obtained by Drude model analysis (solid lines).

ture, we fitted the real and imaginary parts of the complex dielectric constant using Drude model

$$\epsilon(\omega) = \epsilon_\infty - \frac{\omega_p^2}{\omega(\omega + i\gamma)}, \quad (2)$$

where  $\epsilon_\infty$  is the dielectric constant at a higher frequency,  $\omega_p$  is the plasma frequency, and  $\gamma$  is the damping constant. Here,  $\omega_p$  and  $\gamma$  are the adjustable parameters. The solid lines in Fig. 2(b) show the best fits for the experimental results. Using this fitting procedure, we determined the plasma frequency and damping constant for all samples with different thicknesses. We also calculated the carrier density by substituting the plasma frequency into  $n = \epsilon_0 m_e^* \omega_p^2 / e^2$ . Here,  $m_e^* \sim 0.005 m_e$  is used as the effective mass in the direction parallel to the electric field of the terahertz wave.<sup>19</sup>

Figure 3(a) shows the estimated carrier density as a function of the film thickness. The thickness dependence of the estimated plasma frequency is also shown in the inset of this figure. The carrier density and plasma frequency dramatically increase with the decrease in the film thickness. Because the ultrathin Bi(001) films have the same crystal structure as a Bi single crystal within our measured range of thickness,<sup>14</sup> the increase in the plasma frequency should be attributed to the change in the dominant electronic states in the carrier dynamics from the bulk to the surface. The estimated value of the carrier density is two orders of magnitude higher than that of the bulk, as shown by a broken line in Fig. 3(a). This difference in the value of the carrier density can be explained by the presence of a surface metallic state that was previously reported in ultrathin Bi(001) films.<sup>2</sup>

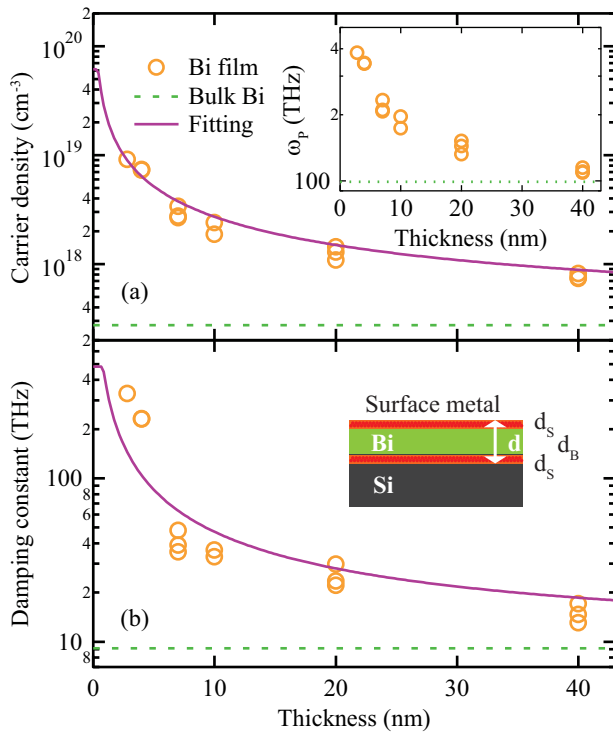


FIG. 3. (a) Carrier density as a function of the film thickness. The inset shows the estimated plasma frequency as a function of the film thickness. (b) Estimated damping constant as a function of the film thickness. The carrier density and damping constant of bulk Bi are shown by broken lines in (a) and (b), respectively.<sup>19,21</sup>

From these results, we conclude that the increases in both the plasma frequency and the carrier density are attributed to a metallic state localized at the surface.<sup>2,20</sup> Because the contribution of the surface component relative to that of the bulk component increases with a decrease in the film thickness, the plasma frequency and the carrier density increase drastically.

In order to discuss the surface metallic state in detail, we estimated the carrier density using the following procedure. The observed Drude dispersion is the average of the semimetal bulk carriers and metallic surface carriers, because the thickness of the film is considerably less than the wavelength of the terahertz wave (effective medium approximation). Then, the carrier density can simply be written as

$$n = n_S \frac{2d_S}{d} + n_B \frac{d - 2d_S}{d}. \quad (3)$$

Here,  $n_S$  is the carrier density at the surface,  $n_B = 2.75 \times 10^{17} \text{ cm}^{-3}$  is the carrier density of the bulk,<sup>19</sup>  $d_S = 0.39 \text{ nm}$  is the thickness of the top bilayer,<sup>14</sup> and  $d$  the total thickness of the ultrathin film. Here, we considered two bilayers for the surface metallic states: the surface of the Bi film and the interface between the Bi film and the Si substrate (see the inset of Fig. 3(b)), because of the weak substrate-film interaction.<sup>2</sup> The result of the fitting is shown by the solid line in Fig. 3(a), and the estimated carrier density of the surface is  $n_S = 3.1 \times 10^{19} \text{ cm}^{-3}$ .

Figure 3(b) shows the thickness dependence of the estimated damping constant. The damping constant also increases with a decrease in the thickness. Assuming the sim-

ilar thickness dependence of the damping constant to that of the carrier density (Eq. (3)) and the bulk damping constant of  $\gamma_B = 9.1 \text{ THz}$ ,<sup>21</sup> the estimated surface damping constant becomes  $\gamma_S = 4.8 \times 10^2 \text{ THz}$  ( $\tau_S = 2.1 \text{ fs}$ ).  $\gamma_S$  represents phase relaxation due to the scatterings at the surface, which includes the surface and the carrier-carrier scattering because of the high carrier density of the surface metallic states. In fact, we found that unlike  $\gamma_B$ ,  $\gamma_S$  is almost independent of temperature, indicating that the temperature-independent carrier-carrier or surface scattering is dominant.

The observed increase in the carrier density and damping constant with an increase in the film-thickness strongly indicates that the surface metallic state dominates the carrier response of Bi thin films. As a result, the SMSC transition might not contribute significantly to the conductive properties of Bi thin films because the surface states have much higher carrier density than the bulk states. Therefore, Bi ultrathin films as a whole always exhibit metallic or semimetallic properties without showing semiconducting behavior.

In conclusion, we have carried out time-domain terahertz spectroscopy for single-crystalline ultrathin Bi(001) films with different thicknesses in the range of 2.8–40 nm. From the results of our study, no gap structure was observed in the terahertz region, owing to which the SMSC transition did not occur in ultrathin Bi films. By analyzing the complex dielectric dispersion of ultrathin Bi films using a Drude model, the plasma frequency and damping constant increased with a decrease in the thickness. The experimental results strongly show the existence of surface metallic states whose plasma frequency and damping constant are quantitatively evaluated. As presented here, broadband THz-TDS is a powerful tool for investigating the carrier dynamics in ultrathin films, owing to which it offers a promising approach to study spin-splitting metallic surface states attributed to the Rashba effect and topological insulators in future.

This work was partially supported by the Ministry of Education, Culture, Sports, Science and Technology through KAKENHI (Grant Nos. 20671002, 21104510, 23241034, and 23104515). I.K. also acknowledges the financial support received through the Special Coordination Funds for Promoting Science and Technology from the Japan Science and Technology Agency (JST).

<sup>1</sup>Y. M. Koroteev, G. Bihlmayer, J. E. Gayone, E. V. Chulkov, S. Blügel, P. M. Echenique, and P. Hofmann, *Phys. Rev. Lett.* **93**, 046403 (2004).

<sup>2</sup>T. Hirahara, T. Nagao, I. Matsuda, G. Bihlmayer, E. V. Chulkov, Y. M. Koroteev, P. M. Echenique, M. Saito, and S. Hasegawa, *Phys. Rev. Lett.* **97**, 146803 (2006).

<sup>3</sup>T. Hirahara, K. Miyamoto, I. Matsuda, T. Kadono, A. Kimura, T. Nagao, G. Bihlmayer, E. V. Chulkov, S. Qiao, K. Shimada, H. Namatame, M. Taniguchi, and S. Hasegawa, *Phys. Rev. B* **76**, 153305 (2007).

<sup>4</sup>L. Fu and C. L. Kane, *Phys. Rev. B* **76**, 045302 (2007).

<sup>5</sup>D. Hsieh, D. Qian, L. Wray, Y. Xia, Y. S. Hor, R. J. Cava, and M. Z. Hasan, *Nature (London)* **452**, 970 (2008).

<sup>6</sup>T. Hirahara, Y. Sakamoto, Y. Saisyu, H. Miyazaki, S. Kimura, T. Okuda, I. Matsuda, S. Murakami, and S. Hasegawa, *Phys. Rev. B* **81**, 165422 (2010).

<sup>7</sup>M. Wada, S. Murakami, F. Freimuth, and G. Bihlmayer, *Phys. Rev. B* **83**, 121310 (2011).

<sup>8</sup>T. Hirahara, G. Bihlmayer, Y. Sakamoto, M. Yamada, H. Miyazaki, S.-i. Kimura, S. Blügel, and S. Hasegawa, *Phys. Rev. Lett.* **107**, 166801 (2011).

<sup>9</sup>Y. F. Ogrin, V. N. Lutskii, and M. I. Elinson, *JETP Lett.* **3**, 71 (1966).

<sup>10</sup>V. B. Sandomirskii, *Sov. Phys. JETP* **25**, 101 (1967).

- <sup>11</sup>C. A. Hoffman, J. R. Meyer, and F. J. Bartoli, *Phys. Rev. B* **48**, 11431 (1993).
- <sup>12</sup>A. Tanaka, M. Hatano, K. Takahashi, H. Sasaki, S. Suzuki, and S. Sato, *Surf. Sci.* **433**, 647 (1999).
- <sup>13</sup>C. R. Ast and H. Hoehst, *Phys. Rev. Lett.* **90**, 016403 (2003).
- <sup>14</sup>T. Nagao, J. T. Sadowski, M. Saito, S. Yaginuma, Y. Fujikawa, T. Kogure, T. Ohno, Y. Hasegawa, S. Hasegawa, and T. Sakurai, *Phys. Rev. Lett.* **93**, 105501 (2004).
- <sup>15</sup>S. Yaginuma, T. Nagao, J. T. Sadowski, A. Pucci, Y. Fujikawa, and T. Sakurai, *Surf. Sci.* **547**, L877 (2003).
- <sup>16</sup>I. Katayama, H. Shimosato, D. S. Rana, I. Kawayama, M. Tonouchi, and M. Ashida, *Appl. Phys. Lett.* **93**, 132903 (2008).
- <sup>17</sup>J. J. Tu, C. C. Homes, and M. Strongin, *Phys. Rev. Lett.* **90**, 017402 (2003).
- <sup>18</sup>I. Katayama, H. Aoki, J. Takeda, H. Shimosato, M. Ashida, R. Kinjo, I. Kawayama, M. Tonouchi, M. Nagai, and K. Tanaka, *Phys. Rev. Lett.* **108**, 097401 (2012).
- <sup>19</sup>G. E. Smith, G. A. Baraff, and J. M. Rowell, *Phys. Rev.* **135**, A1118 (1964).
- <sup>20</sup>T. Hirahara, I. Matsuda, S. Yamazaki, N. Miyata, and S. Hasegawa, *Appl. Phys. Lett.* **91**, 202106 (2007).
- <sup>21</sup>E. Gerlach, P. Grosse, M. Rautenberg, and W. Senske, *Phys. Status Solidi* **75**, 553 (1976).